UNIVERSITY OF BUCHAREST
FACULTY OF PHYSICS

PRODUCTION STUDIES OF Λ_b BARYONS AT LHCB

– Summary of the thesis –

PhD candidate,
Bogdan Paul Popovici

PhD adviser,
Prof. Dr. Sabin Stoica

2011

Abstract

This thesis contains the main results obtained by the author during his participation in the Large Hadron Collider beauty (LHCb) collaboration as member of the Romanian LHCb group. They refer to contributions obtained both during the construction period of the LHCb detector and after the start of the Large Hadron Collider (LHC) and of the LHCb experiment.

The thesis is structured into five chapters and one Annex. In the first Chapter - Introduction, a general view of the Standard Model (SM) and its limitations are presented, together with the general motivation for the LHC, and particularly, for the LHCb searches. In Chapter 2, the theoretical tool used in SM cross section calculations, i.e. the perturbative Quantum Chromodynamic (pQCD), is shortly described, together with the phenomenology of the b quark production and Λ_b physics, with the goal of a better understanding of the context in which the main contribution of this thesis falls into. In the third Chapter, a detailed description of the LHCb detector and its sub-detectors is presented, aiming to provide the reader with more detailed information about the detector's performances and the type of events that can be searched for within the LHCb experiment. Chapter 4 presents the contribution of the author to the development of a calibration method for the RICH subdetectors, which turned out to be very useful in order to fully exploit its performances for hadron identification over the wide momentum range, from 2 to 100 GeV/c. Further, the method is applied to the case of the measurement of Λ_b production.

The main contribution of this thesis is described in Chapter 5 and consists in a complete analysis of a measurement of the Λ_b^0 production cross section at 7 TeV in hadronic events at LHCb experiment. Using the data collected in 2010, of $35pb^{-1}$, the total cross section was measured after the reconstruction of the decay chain, $\Lambda_b^0 \to J/\psi(\mu^-\mu^+)\Lambda^0(p\pi^-)$, using several methods of selecting different types of tracks for the "stable" particles.

Another original contribution, presented in Annex, refers to writing a software package which can be generically used in other similar data analyzes. Other contributions related to the participation of the author in the monitoring of the data acquisition by the LHCb detector and in offline checking of the data quality are also mentioned.

In the following, we shortly describe the content of each chapter, highlighting the original contributions and the references they have been reported in.

1 Introduction

The Standard Model (SM) is a theory of elementary particles and the way they interact through the electromagnetic, weak, and strong forces. Developed in the 1970s, it incorporated all the elementary particles known at that time, but also it correctly predicted the existence and the properties of new ones which were later discovered. The charm, bottom and top quarks, the tau neutrino, the $W^{\pm}$ and Z bosons and the gluon were predicted before they were discovered. The last predicted but still undiscovered particle, the Higgs boson, is now almost to be confirmed, after the discovery of a new particle with its characteristics reported at LHC in August 2012 [1].

The SM particles are classified in i) fermions, particles with half-integer spin that obey the Fermi-Dirac statistics, which are the building blocks of the matter (there are twelve fermions - six quarks and six leptons), and ii) bosons, particles with integer spin that obey the Bose-Einstein statistics, which are the carriers of forces (there are six bosons). There are three generations of leptons, each of them consists of a charged particle (electron, muon, tau) and a neutral partner (electron, muon and tau neutrinos). In an analogous manner, three generations of quarks exist, each consisting of a charge $+2/3e$ quark (up, charm and top) and a charge $-1/3e$ quark (down, strange and bottom). The generations are arranged according to a mass hierarchy which is not completely understood. As for the carriers of forces, the gluons mediate the strong interactions, the $W^{\pm}$ and Z bosons mediate the weak interaction, and the photon the electromagnetic one. The strong interaction is achieved through the 8 mediators called gluons which carry the property of colour (see the Table 1 for a complete view of the elementary particles, the carriers of forces and of their properties).

With these particles one can build composite particles, hadrons - particles made up of multiple quarks bound together, as follows: i) baryons (fermions) - particles composed of three quarks (like nucleons or hyperons) and ii) mesons (bosons) - particles composed of a pair quark-antiquark. Further, atomic nuclei are formed by protons and

	Particles	Mass [MeV/c^2]	Spin	Charge/e^+	Colour states
quarks	down (d)	4-8	1/2	-1/3	3
	up (u)	1.5-4	1/2	2/3	3
	strange (s)	80-130	1/2	-1/3	3
	charm (d)	$(1.15 - 1.35) \cdot 10^3$	1/2	2/3	3
	bottom (b)	$(4.1 - 4.9) \cdot 10^3$	1/2	-1/3	3
	top (t)	$1.74 \cdot 10^6$	1/2	2/3	3
leptons	e^-	0.511	1/2	-1	0
	ν_e	$< 3 \cdot 10^{-6}$	1/2	0	0
	μ^-	105.66	1/2	-1	0
	ν_μ	< 0.19	1/2	0	0
	τ^-	1777	1/2	-1	0
	ν_τ	< 18.2	1/2	0	0
gauge bosons	γ	0	1	0	0
	$W^\pm$	$80.41 \cdot 10^3$	± 1	0	0
	Z	$91.18 \cdot 10^3$	1	0	0
	gluon (g)	0	1	0	8
	Higgs (H)	$> 114 \cdot 10^3$	0	0	0
	Graviton (G)	0	2	2	0

Table 1: Particles of the minimal Standard Model: the first group contains quarks, the second, leptons, and the last one, gauge bosons. All charges are given in units of positron charges. The gravitational force is also considered. The graviton and Higgs boson are the last two un-observed particles.

neutrons, and atoms - the basic chemical building block of matter - are composed of electrons, protons, and neutrons. Mathematically, the relativistic quantum field theory (QFT) is the adequate theoretical framework to formulate the SM [2]. It is a gauge invariant QFT based on the symmetry group $SU(3) \otimes SU(2) \otimes U(1)$, with the colour group SU(3) for the strong interaction and with $SU(2) \otimes U(1)$ for the electroweak interaction spontaneously broken by the Higgs mechanism. In the language of gauge theories the basic structures are the fields, the fields of matter of half-integer spin and of those which carry the interaction, of integer spin.

The strong interaction part is described by the Quantum Chromodynamic, which is a renormalizable theory, allowing one to consistently

define the perturbative calculations. However, due to the large values of the strong coupling constant, perturbative calculations in higher order are difficult to make and finding an appropriate way to sum such terms is a long standing problem in perturbative Quantum Chromodynamic (pQCD).

The Standard Model is a very robust theory tested in numerous experiments in the past 40 years, but it does not address a series of open problems, like the explanation for the mass hierarchies, the inclusion of the gravitational interaction into the model, and other experimental observations from astrophysics, such as, dark matter, the disparity between matter and antimatter etc.

There are strong indications from within the theory of SM itself, that new phenomena should be expected at the level of TeV scale, and this represents one of the important reasons why the LHC accelerator, and large experiments around it were built to search for them in pp collisions at energies ranging from 7 TeV up to 14 TeV.

LHCb is one of these experiments, whose main purpose is to look at indirect evidences of New Physics through the study of very rare decays of b and c-flavored hadrons, and precision measurements of CP-violating observables. No surprise however, the LHCb is able to contribute to a larger physics program, testing the SM and providing new tools for understanding the current theories and their limitations. One of such direction is to test pQCD calculations, which covers the area where the main contribution of this thesis falls into. Since events which contain hadrons with b quarks represent an important background in many different analyzes, studies of the rates of production for such events are interesting on a general level.

2 QCD and b quark production. Λ_b phenomenology

In current collider experiments the hard interaction of two incoming beams results in the production of up to thousands of outgoing particles. So far, no evidence has been found to contradict the belief that

this process is described by the SM for strong and electroweak phenomena. Unfortunately, a full quantum-mechanical treatment is out of reach. There are two reasons for this apparent shortcoming: first of all, the sheer number of particles involved gives rise to a tremendous number of interfering contributions that grows factorially with the number of particles. Furthermore, perturbation theory alone is not able to account for some important phenomena, such as the transition of partons to hadrons. Factorization theorems are then used to split the contribution of short range interactions, subject to the perturbative regime, from the long range interactions, which are accounted for phenomenological models fitted from experimental observations. Combining these two approaches, simulation tools called Monte Carlo programs or event generators have proved to be successful for a detailed description of multiparticle production.

2.1 QCD and perturbative calculations

In hadron-hadron interactions heavy quarks ($Q = c, b$) are produced in the hard collisions of a parton from each hadron. The general form of the heavy quark production cross section in collisions between hadrons A and B is [3]

$$\sigma(s) = \sum_{i,j} \int dx_A dx_B d\hat{\sigma}_{ij}(x_A x_B s, m^2, \mu_1^2) F_i^A(x_A, \mu_2) F_j^B(x_B, \mu_2) \quad (1)$$

where $\sqrt{s}$ is the total center of mass energy of the $A+B$ hadron system, F_i^A are the structure functions which measure the probability of parton i in hadron A to carry fractional momentum x_A, m is the heavy quark mass, μ_1 and μ_2 are the normalization and factorization scales, and $d\hat{\sigma}_{ij}$ is the short distance partonic cross section for the process $ij \to Q\bar{Q}X$ which occurs at the effective center of mass energy

$$\hat{s} = x_A x_B s.$$

The terms involved in calculating $d\sigma(s)$ can not be calculated exactly. Instead, they are expanded into a perturbative power series in the

strong coupling constant α_s

$$d\hat{\sigma}_{ij}(\hat{s}, m^2, \mu_1^2) = \alpha_s^2(\mu_1) f_{ij}^{(0)}(\hat{s}, m^2) + \alpha_s^3(\mu_1) f_{ij}^{(1)}(\hat{s}, m^2) + \dots \quad (2)$$

$$F_i^A(x_A, \mu_2) = g_i^{A,(0)}(x_A, \mu_2) + \alpha_s(\mu_2) g_i^{A,(1)}(x_A, \mu_2) + \dots \quad (3)$$

where the functions f, g and the constants μ_1, μ_2 depend upon the scheme used for renormalization and factorization. The indexes (0) and (1) refer to the leading order (LO) and next to leading order (NLO) terms respectively.

To calculate the total heavy quark production cross section is then an exercise in determining the partonic cross section derived to some order in α_s, and convoluting them with the structure functions. This technique was followed using complete $\mathcal{O}(\alpha_s^3)$ calculations by Nason, Dawson and Ellis (NDE) [3, 4].

The previous fixed order calculation is reasonable when the heavy-quark mass is the only relevant mass scale of the specific process, and it fails when the transverse momentum of the heavy quark is much larger than its mass. In that case, the order of neither the heavy quark mass nor the transverse momentum can be chosen as the renormalization and factorization scales, since the large logarithms in terms of $\alpha_s^2(\alpha_s \log \frac{p_T}{m})^n$ (LL) and $\alpha_s^3(\alpha_s \log \frac{p_T}{m})^n$ (NLL) break the convergence. An approach for treating this problem was proposed in Ref. [5], where the terms to be summed are redistributed between the perturbative and non-perturbative factorization terms. This was, however, only a first step since it was a "massless" approach. The development of the resummation idea and the fixed order calculations led to the development of FONLL method [6] whose general strategy can be written as

$$\text{FONLL} = \text{FO} + (\text{RS} - \text{FOM0}) \times G(m, p_T) \quad (4)$$

where FOM0, the massless limit component, corresponds to the fixed order (FO) terms in the resummation (RS) calculation, which should be subtracted to avoid double counting. A matching procedure is introduced to match the RS and the FOM0 calculations. The function $G(m, p_T)$ is quite a general one, it has to approach unity $\frac{m}{p_T} \to 0$ and to suppress the logarithm terms in the low p_T range. The result from

this method can then be described as

$$\frac{d\sigma}{dp_T^2} = A(m)\alpha_s^2 + B(m)\alpha_s^3 + \\ +(\alpha_s^2 \sum_{i=2}^{\infty} a_i(\alpha_s \log\frac{\mu}{m})^i + \alpha_s^3 \sum_{i=2}^{\infty} b_i(\alpha_s \log\frac{\mu}{m})^i) \times G(m, p_T) \quad (5)$$

where coefficients $a(m)$ and $b(m)$ are extracted from the LO and NLO calculations and the coefficients a_i and b_i depend on the colliding center of-mass energy s, p_T and scales μ.

2.2 Monte Carlo simulation

The previous theoretical method addressed the perturbative part of the problem and it relies on different experimental input and phenomenological methods to account for parton distribution function or hadronization functions. This procedure can be sometimes difficult and not optimal if we are interested in new models, or we worry about the computational time. Thus general frameworks have been developed to generate events for simulation studies. These event generators treat the full process of collision, the hard interaction of the partons, the emission of the radiation, the formation of jets, hadronization, underlying events. Currently, the most used event generators are Pythia [7], Herwig++ [8] and Sherpa [9], which propose alternative solutions for the splitting mentioned above and are useful for making comparisons. They are built as modular packages which can be sometimes interchanged between themselves and, more important, have interfaces that allow the implementation of a specific phenomenon in a easy manner when new solutions are proposed. However, they are still under development and sometimes they have not implemented specific processes, or their very core idea cannot be easily made compatible with the theoretical ones. For instance, with respect to the hard interaction, all generators offer LO calculation but not necessarily NLO calculations, while the FONLL scheme is not fully implemented in either of them. Careful evaluation has to be made when choosing a generator for a

specific problem, or when interpreting the differences between their predictions.

For this thesis we used Pythia event generator and also compared the results with the prediction from FONLL calculation from [6], and NLO prediction from POWHEG [10].

2.3 Λ_b phenomenology

The main result of this thesis is the measurement of the production cross section of the Λ_b baryon in pp collision at 7 TeV within LHCb collaboration. This follows the interest of testing the validity of pQCD calculations at these new energies and in a unique phase space for the baryons which contain the b quark. The decay mode chosen for this is $\Lambda_b^0 \to J/\psi\Lambda^0$, see Fig. 1, which although not the most abundant, has the advantage that can be well reconstructed and relates tightly to a list of other interesting applications. The present analysis is part of a more general program which motivates our work and which includes: i) spectroscopy; measurement of masses, lifetime, states, confirming Λ_b^0 decay modes; ii) relative production rate measurement of baryons; iii) baryon fragmentation factor f_{baryon}; iv) polarization studies $\Lambda_b^0 \to J/\psi\Lambda^0$; v) CP violation in direct searches $\Lambda_b^0 \to J/\psi\Lambda^0$; vi) time reversal violations $\Lambda_b^0 \to J/\psi\Lambda^0$; vii) SM checks in radiative decays $\Lambda_b^0 \to \Lambda^0\gamma$; viii) search for charmless hadronic b-meson decays; ix) forward production of beauty baryons in pp collisions [11, 12]. The production of the Λ_b baryons is an important step of this program since it provides us with the basic tools for performing these studies.

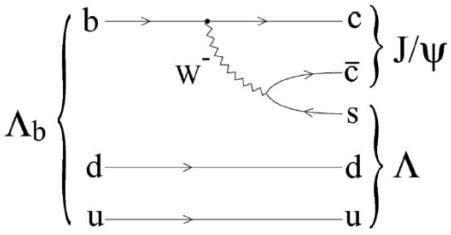

Figure 1: Feynman diagram for the weak Λ_b decay.

3 The LHCb experiment

The LHCb detector [13], see Fig.2, is a single-arm forward spectrometer covering the pseudorapidity range $2 < \eta < 5$, designed for the study of hadrons containing b or c quarks. The spectrometer includes a high precision tracking system consisting of a silicon-strip vertex detector (VELO) surrounding the pp interaction region, a large-area silicon-strip detector located upstream of a dipole magnet with a bending power of about 4 Tm, and three stations of silicon-strip detectors and straw drift-tubes placed downstream. The combined tracking system (trigger tracker-TT, and the tracking stations T1-T3) has a momentum resolution $\Delta p/p$ that varies from 0.4% at 5 GeV/c to 0.6% at 100 GeV/c, and an impact parameter (IP) resolution of 20 μm for tracks with high transverse momentum. Charged hadrons are identified using two ring-imaging Cherenkov detectors (RICH). Photon, electron and hadron candidates are identified by a calorimeter system consisting of scintillating-pad (SPD) and preshower detectors (PS), an electromagnetic calorimeter (ECAL) and a hadronic calorimeter (HCAL). Muons are identified by a system composed of alternating layers of iron and multiwire proportional chambers (M1-M5). An instrumental bias can be caused by the vertical magnetic field, which deflects oppositely-charged particles into different regions of the detector. This potential bias is experimentally reduced by regularly changing the polarity of the magnetic field during data taking. The data used in this analysis were recorded with both magnet polarities in almost equal amounts.

To select the physical events there is a trigger system which consist of two parts: i) the Level0 (L0) and ii) the High Level Trigger (HLT). They have been optimized to maximize the signal to noise ratio during data taking. L0 trigger is a hardware device based on information from the calorimeter and muon systems. The HLT is a two level software application (HLT1 and HLT2) running in a computer farm which apply a full event reconstruction. Events analyzed here pass a hardware trigger which requires either one muon candidate with a p_T larger than 1.4 GeV/c, or two muons with p_T larger than 0.56 GeV/c and 0.48 GeV/c, respectively. For the purpose of the analysis described in

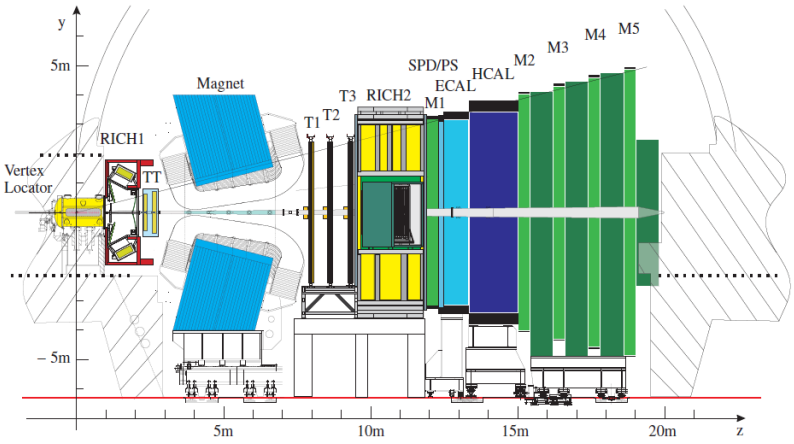

Figure 2: LHCb detector

Chapter 5, the software trigger [14] selects high transverse momentum muons, $p_T > 1.8\ GeV/c$, or softer ones, $p_T > 0.8\ GeV/c$, accompanied by another track with which they can form a secondary vertex. In the latter case both the muon and the second accompanying track undergo further quality cuts which require a momentum $p_{tot} > 8\ GeV/c$ and an IP with respect to any primary pp interactions larger than 110 μm. A successive stage of the software trigger accepts only events in which the muon and the track, also assumed to be a muon, have a combined invariant mass within 120 MeV/c^2 of the nominal J/ψ mass. In order to remove events that, in processing, would require too much CPU time, a set of Global Event Cuts (GEC) based on sub-detector multiplicities is applied at the beginning of each trigger stage.

The measurement presented in Chapter 5 is based only on events in which the trigger selected muons are originating from the J/ψ produced in the Λ_b^0 decay, the so called Trigger On Signal (TOS) events. It is however possible that the trigger selects events independently of the Λ_b^0 daughters, Trigger Independent of Signal (TIS) events. TIS and TOS requirements are not mutually exclusive and are used to estimate the efficiency of the trigger as it will be shown later.

The data collected by the detector at the runtime are stored into large computer farms distributed in a network called GRID, which is

spread around participating laboratories organized in tiers. Further processing steps run both by the collaboration and by the end-user prepare the data for the offline analysis. ROOT [15], written in $C++$ is the general software framework used in experimental particle physics for offline analysis. For this thesis we have written a Python package which implements the steps of the analysis. This package, described in Annex, can/and has been used by other people in their analyzes.

We also used data from simulated events for the calibration method or total efficiency estimation for example. The pp collisions are generated using PYTHIA 6.4 [7] with a specific LHCb configuration [16]. Decays of hadronic particles are described by EvtGen [17] in which final state radiation is generated using PHOTOS [18]. The interaction of the generated particles with the detector and its response are implemented using the Geant toolkit [19] as described in Ref. [20].

4 MC free calibration of LHCb RICH detectors using the $\Lambda \to p\pi$ decay

The RICH detectors provide hadron identification over the wide momentum range from 2 to 100 GeV/c, and are central to the physics goals of the LHCb experiment. An excellent understanding of the hadron identification performance of the RICH detectors is essential. To achieve this goal, calibration strategies have been devised to enable the measurement of the performance from the real data. In this context, a calibration method for selecting high purity samples of Λ's was first implemented at LHCb by the author. This method, described in the present Chapter, is applied to evaluate the particle identification (PID) performance of pions and protons.

4.1 RICH calibration with $\Lambda^0 \to p\pi^-$ decay

For both offline physics analyses and online data monitoring, the ability to understand the performance of the RICH particle identification (PID) in a Monte Carlo independent manner is of vital importance. In

order to achieve that, signals which can be reconstructed without the inputs from the RICH have been looked for. If these signals can be very well isolated from the background we will obtain unbiased samples of identified final particles and thus we can evaluate the PID response from the detectors.

The method consists in developing a set of requirements in order that the signal be isolated from background. We proved that the method is efficient for $\Lambda \to p\pi^-$ decay, being thus useful for the identification of the protons and pions. The same algorithm can be applied for other neutral resonances which decay into two charged particles. Thus, the method was extended to other resonances like $K^0_S \to \pi^-\pi^+$ for pions and $J/\psi \to \mu^+\mu^-$ for the muons. One can mention that the method can also be adapted for kaons with the decay $\phi \to K^+K^-$. The method also has the advantage that it uses particles abundantly produced in minimum bias events, which makes it useful in the online monitoring.

The selection employed makes use of the properties of the Λ^0 which decays weakly and has a long lifetime, a path of a few centimeters in the detector; also the fact that the mass of Λ^0, $m_{\Lambda^0} = 1115.6\ MeV/c^2$, is very close to the proton mass, $m_{\Lambda^0} = 938.2\ MeV/c^2$; allows one to identify the proton from pion. The reconstruction algorithm selects the combination of two charged tracks which pass a list of conditions. The most energetic track was assumed to be the proton and the second the pion. Then, the condition for selecting secondary particles, i.e. not originating from the primary vertex, was imposed, $\chi^2_{IP}(\pi) > 13$ and $\chi^2_{IP}(p) > 6$. The condition on the transverse momenta was left almost untouched since we would like to extend the range of the method to lower momenta, $p_T(\pi) > 0.1\ GeV/c$ and $p_T(p) > 0.5\ GeV/c$. The two tracks were asked to form a vertex with higher probability, $\chi^2_{vtx}(\Lambda^0) < 10$, and then the distance from the primary vertex to the decay vertex was asked to be significant $\chi^2_{flight}(\Lambda^0) > 10$. The last condition imposed a narrow cut on the invariant mass of the reconstructed Λ^0, $|m(p\pi) - m_{PDG}(\Lambda^0)| < 1.5\ GeV/c^2$ since we are less interested in optimizing the total efficiency but rather the purity.

In Fig. 3, the plot in the middle, we see the invariant mass of pairs

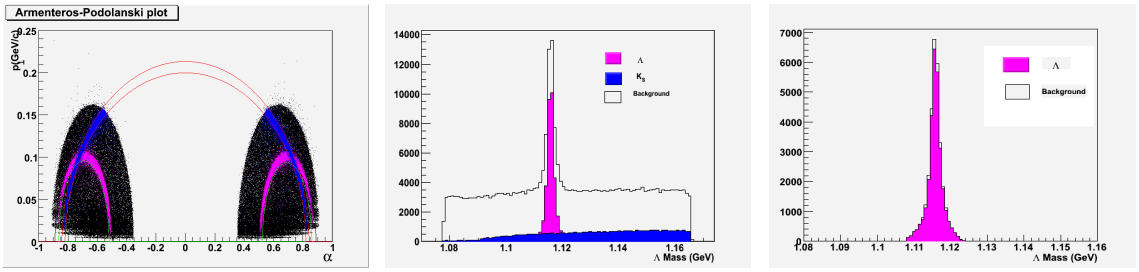

Figure 3: Left plot represents the data in Armenteros-Podolanski variables. Middle and right plots show the data in $p\pi$-invariant mass variable, before, and after applying the full selection; magenta - true $\Lambda/\bar{\Lambda}$, blue - true K_S, black - all combinations,

of tracks that were given the mass of proton and pion respectively. Without imposing the above cuts, the peak is already well shaped but sits on a large combinatorial background. Also, misidentified pions coming from K_s produce a contamination of Λ^0 peak. For improving the above selection and also for rejecting the K_S background from the sample we use the Armenteros-Podolanski variables [21]. This amounts to the following change of the variables $(p_p, p_\pi, \cos\theta_{p\pi}) \rightarrow (p_\perp, \alpha, 1/P_\Lambda)$, where: $\alpha = \frac{p_{p||} - p_{\pi||}}{P_\Lambda}$, $P_\Lambda = p_{p||} + p_{\pi||}$; $p_\perp$, $p_{p||}$, $p_{\pi||}$ are defined relative to P_Λ direction.

The representation of the candidates in $p_\perp$ and α variables is shown in Fig. 3. The plot distinctly shows how the signal and background are separated.

The Λ^0 and K_S^0 shapes can be explained by rewriting the energy-momentum relation

$$p_\perp^2 + \frac{(\alpha - \alpha^*)^2}{4(1/M_\Lambda^2 + 1/P_\Lambda^2)} = p^{*2} \tag{6}$$

with $\alpha^* = \frac{m_p^2 - m_\pi^2}{M_\Lambda^2}$, p^*- momentum of the decay products in the C.M.S.

Then, the elliptic curves suggested by Eq. 6 are used to fit the signal region and select the true Λ^0 candidates.

4.2 Identification efficiency plots

The method described earlier gives excellent results for the purity of the sample of protons (96%) and pions (98%). This shows the validity of the method, see also Fig. 3, right side for a plot of the invariant mass. The identification performances of this method are then evaluated as function of the momentum of the proton/pion. Identification/mis-identification efficiency curves for RICH, as they are simulated by Monte Carlo, are very well described by the efficiency curves obtained using data, see Fig. 4.

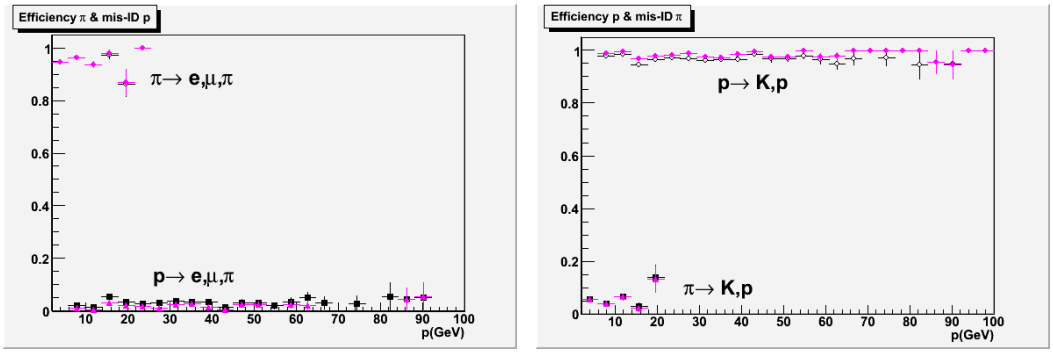

Figure 4: Black - pions and protons selected using kinematic cuts; Magenta - truth pions and truth protons selected using the same cuts. Up - identification efficiency curves; down - misidentification efficiency curves. Pions/protons are seen by the RICH as light (e, μ, π) particles or/and heavy (K, p) particles.

The results of this method were presented in a public conference [1] and used for calibrating the RICH detectors at LHCb. For example such calibration was used for evaluating the systematic uncertainties in the analysis from Chapter 5 of the Λ_b production. Further use of these studies contributed to the publication of some of the first LHCb papers concerning prompt K_s^0 production at $\sqrt{s} = 0.9$ TeV [2], the measurement of V^0 production ratios at $\sqrt{s} = 0.9$ and 7 TeV [3], or the measurement of prompt hadron production ratios [4]. A summary

of these first results of LHCb, concerning soft physics, can be found in [5].

5 Measurement of Λ_b production at 7 TeV

The study of b quark production is an important topic at LHC as a test of QCD, for the presence of b quark in many interesting physics topics like CP-violation or the discovery of new heavy particles. The production of the b-baryons is a less explored territory, as they could not be produced at B-factories and few results have been reported by the Tevatron experiments. This chapter presents a measurement of the Λ_b cross-section in the decay channel $\Lambda_b \to J/\psi(\mu^-\mu^+)\Lambda^0$ in the region $p_T < 13.0\ GeV/c$ and $2.2 < y < 4.5$, using $36.4 \pm 1.3\, pb^{-1}$ of data recorded by the LHCb detector in 2010. In the three sections of this chapter the cross-section measurement, the systematic uncertainties and the final results are presented.

5.1 Cross-section measurement

Selection criteria, defined for the measurement of the Λ_b lifetime with the LHCb detector [22], are applied to all final state particles identified as p, π, μ^- as well as to the reconstructed J/ψ, Λ^0, and Λ_b. A full list is shown in Table 2. Given the long lifetime of the Λ final state, the pion and proton can be reconstructed either as a pair of tracks that leave a signal in the VELO, long tracks, or as one that is detected only in the subsequent tracking stations, downstream tracks. In order to maximize the statistical significance of the present measurement both Λ reconstructed with long tracks and Λ reconstructed with downstream tracks are used to measure Λ_b production cross section. These two samples are analyzed separately as they are subject to different experimental systematic effects. For similar reasons the data set is further split according to the b-quark content of the Λ_b and to the polarity of the magnetic field.

The number of candidates of Λ_b signal is estimated by means of an unbinned fit of the invariant mass distribution in each of the eight sam-

Table 2: Requirements used to select first the $J/\psi \to \mu^+\mu^-$ then the $\Lambda^0 \to p\pi^-$ and finally the $\Lambda_b^0 \to J/\psi\Lambda^0$ candidates. M and m are used to indicate the measured invariant masses and the nominal masses respectively. As the Λ^0 can be reconstructed from a pair of long tracks (LL) or downstream tracks (DD) different values are indicated where applied, τ is the decay time of the particle and IP_{χ^2} the difference in the χ^2 of the primary vertex measured with and without the respective track. The K_S^0 background is eliminated from the Λ^0 sample by applying a requirement on $|M_{\pi^-\pi^-} - m_{K_S^0}|$.

Decay mode	Parameter	Value
$J/\psi \to \mu^+\mu^-$	$p_T(\mu^+)$, $p_T(\mu^-)$	> 0.5 GeV/c
	$\lvert M_{\mu^+\mu^-} - m_{J/\psi_{PDG}}\rvert$	$< 55\mathrm{MeV}/c^2$
$\Lambda^0 \to p\pi^-$	$\mathrm{IP}_{\chi^2}(p,\pi)$	> 9(LL), 4(DD)
	$p_T(\pi^-)$	> 0.1GeV/c
	$p_T(p)$	> 0.5GeV/c
	$p(p,\pi^-)$	> 2GeV/c
	$\lvert M_{p\pi^-} - m_{\Lambda^0}\rvert$	$< 6 MeV/c^2$
	$\lvert M_{\pi^-\pi^-} - m_{K_S^0}\rvert$	> 8(LL), 14(DD)MeV/c^2
	$p_T(\Lambda^0)$	> 1GeV/c
$\Lambda_b^0 \to J/\psi\Lambda^0$	$M_{\Lambda_b^0}$	$\in (5120, 6120)\mathrm{MeV}/c^2$
	IP_{χ^2}	< 20
	$\tau(\Lambda_b^0)$	> 0.25 ps

ples. The signal is assumed to be distributed as a Gaussian function while the background is described by a first order polynomial function. The Λ_b^0 and $\bar{\Lambda}_b^0$ samples are grouped in four pairs according to the track type and magnet polarity. These pairs are fitted simultaneously with the constraint that the mean value and the variance of the Gaussian function are the same. As an example Fig. 5 shows the results of the fits of the $\bar{\Lambda}_b^0$ invariant mass distributions. The fits yield a total of 229 $\pm$ 51 signal events in the eight samples.

The *sPlot* technique [23] is used to estimate a statistical weight w_{SP} for each candidate. This weight is related to the probability of the candidate to be a true signal candidate based on the fit model. The efficiency corrected number of $\Lambda_b^0 \to J/\psi\Lambda^0$ decays is then calculated

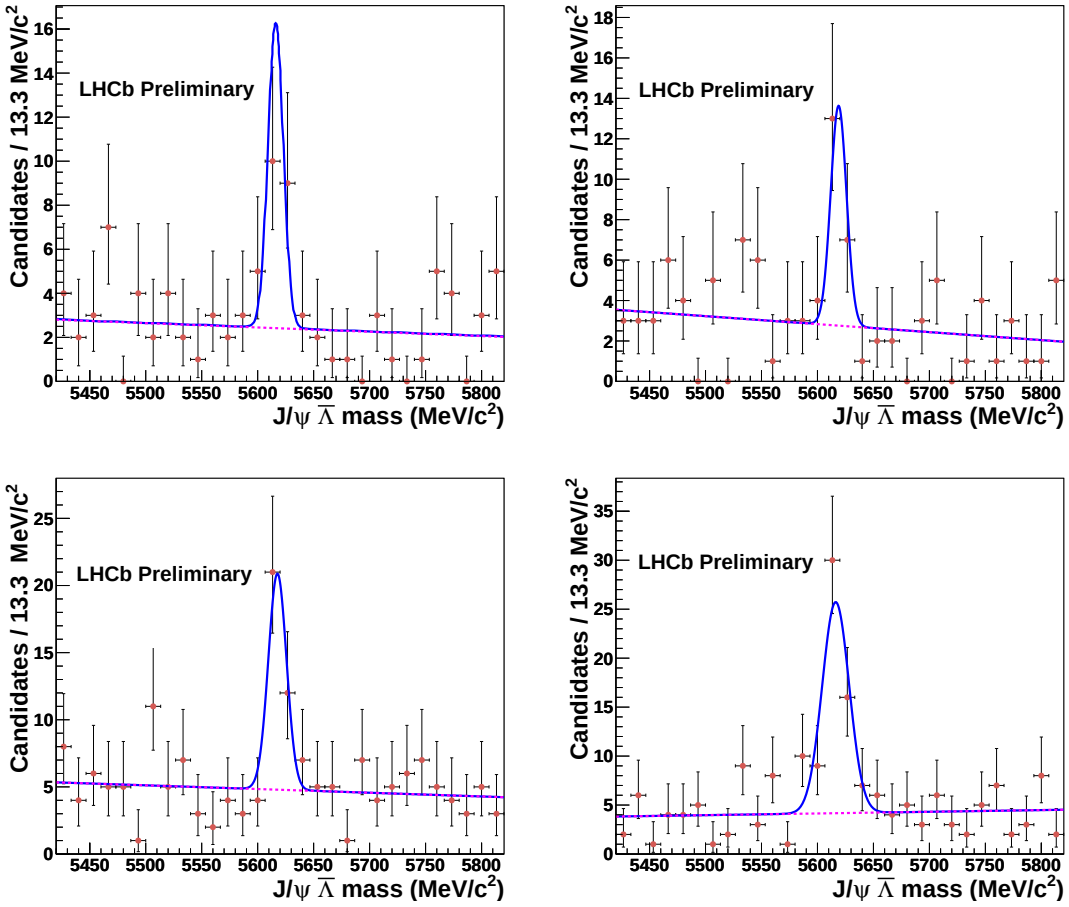

Figure 5: $\bar{\Lambda}_b^0 \to J/\psi \bar{\Lambda}^0$ mass fit. Top: $\bar{\Lambda}$ is reconstructed using long tracks. Bottom: using the downstream tracks. The plots on the left and on the right used data recorded with different magnet polarities.

by weighting each candidate with

$$w_{\rm TOT} = \frac{w_{\rm SP}}{S \times \epsilon^{\rm rec} \times \epsilon^{\rm trig}} \tag{7}$$

where S is a scale factor related to the GEC and to the differences between data and the simulation that are not taken into account in the efficiency determination, $\epsilon^{\rm rec}$ combines the acceptance, detection, reconstruction and selection efficiencies while $\epsilon^{\rm trig}$ is the trigger efficiency. The weighted yield obtained in this way is used to estimate the total number of $\Lambda_b^0 \to J/\psi \Lambda^0$ decays, $N^{\rm corr}_{\Lambda_b^0}$.

The value of $\epsilon^{\rm rec}$ is measured as a function of p_T and y for each of the eight categories of Λ_b^0 candidates using fully simulated samples of $\Lambda_b^0 \to J/\psi\Lambda^0$ signal decays. The simulated p_T and y distributions are reweighted event-by-event to account for the different track multiplicity and the distribution of the events over the phase-space observed in data.

The trigger efficiency has been determined from data by means of the procedure described in [24] and is defined as:

$$\epsilon^{\rm trig} = \frac{1}{1 + \frac{N_{J/\psi}^{\rm TIS\cancel{TOS}}}{N_{J/\psi}^{\rm TISTOS}}} \tag{8}$$

where $N_{J/\psi}^{\rm TIS\cancel{TOS}}$ is the number of J/ψ candidates detected, reconstructed, and selected by the J/ψ specific selection criteria, which pass the TIS but not the TOS criteria and $N_{J/\psi}^{\rm TISTOS}$ is the number of corresponding J/ψ candidates which pass both TIS and TOS criteria. A data-set enriched in J/ψ mesons has been used to estimate these numbers of J/ψ candidates as function of the J/ψ rapidity and transverse momentum and magnet field polarity.

The scale factor S is equal to 0.984 ± 0.006 and it includes several factors. The first takes into account the loss in efficiency due to the global event cuts, 0.973 ± 0.006. The muon identification efficiency is found to be greater in data than in simulation, introducing a correction factor 1.024 ± 0.012. Analogously the vertex reconstruction efficiency is found to be smaller in data by 0.984 ± 0.008.

Two different techniques [25] are applied to measure the integrated luminosity of the data sample. In addition to the Van der Meer scan method, LHCb also exploits the proximity to the beam and the high resolution of the VELO subdetector to measure beam parameters such as positions, angles and widths in beam-beam and beam-gas interactions. Combining the results of both techniques it is possible to measure the integrated luminosity over the whole data taking period used in this analysis with an uncertainty of 3.5%, obtaining 36.4 ± 1.3 pb^{-1}.

The estimated $N_{\Lambda_b^0}^{\rm corr}$ together with the information on luminosity and branching fractions provide eight measurements of the cross-

Table 3: Systematic uncertainties for the cross-section measurements in percent. Where the uncertainty is different for the eight sub-samples in which the candidates are divided, the smallest and the largest estimated values are shown. The total systematic uncertainty is obtained assuming total correlation among the correlated variables.

Source of systematic uncertainties	Value (%)
GEC	0.60
trigger efficiency	2.23 – 4.48
tracking efficiency	3.26 – 4.47
reconstruction efficiency	2.59 – 7.60
primary vertex efficiency	0.79
selection	0.13 – 1.94
muon particle identification	1.12
proton particle identification	0 – 0.56
fitting model	0.26 – 7.70
crossing angle	0.02 – 0.31
polarization	0.29 – 3.74
luminosity measurement	3.50
branching fractions	1.00
Total	10.9 – 21.9

section according to

$$\sigma(pp \to \Lambda_b^0 X)\mathcal{B}(\Lambda_b^0 \to J/\psi\Lambda^0) = \frac{N_{\Lambda_b^0}^{\rm corr}}{\mathcal{L} \cdot \mathcal{B}(\Lambda^0 \to p\pi^-)\mathcal{B}(J/\psi \to \mu^+\mu^-)} \tag{9}$$

where $\mathcal{L}$ is the luminosity, $\mathcal{B}(\Lambda^0 \to p\,\pi^-)$ and $\mathcal{B}(J/\psi \to \mu^+\mu^-)$ are the branching fractions of the $\Lambda^0 \to p\pi^-$ and $J/\psi \to \mu^+\mu^-$ decays averaged by the PDG [26].

5.2 Systematic uncertainties

A number of systematic effects are studied, and their impact on the cross-section measurement is quantified.

A systematic uncertainty associated to the selection of the Λ_b^0 candidates is assigned varying the requirements listed in Table 2 by the error on the cut variable. To estimate the uncertainties introduced by the fit procedure, the Λ_b^0 samples are grouped in different ways and alternative constraints are imposed on the mean and variance of the Gaussian function used in the fit. A different model, where the background is described by an exponential, has also been tested.

Systematic uncertainties due to the errors on $\epsilon^{\rm trig}$, to the limited statistics of the simulated samples used to determine $\epsilon^{\rm rec}$, as well as to the differences between data and simulation are evaluated using a series of pseudo-experiments. The difference in the material description in data and simulation is treated separately and an additional systematic uncertainty is assigned to each track to account for it. Further contributions to the systematic uncertainties are introduced by the statistical error on the GEC efficiency determined from data, the difference between data and the simulated samples in the primary vertex reconstruction efficiency, the muon and proton particle identification efficiencies and the beam collision geometry.

The uncertainty introduced in the production measurement by the lack of knowledge on the Λ_b^0 polarization is estimated considering a transverse polarization and comparing the two extreme cases for the polarization, ± 1, with the nominal measurement where the Λ_b^0 is assumed to be unpolarized.

The complete list of systematic uncertainties considered in this analysis, including the errors on the luminosity and on the theoretical values for the branching fractions of the decays considered, is shown in Table 3. All uncertainties are combined to provide a final systematic uncertainty. Where correlation is possible, maximum correlation is assumed.

Summary and results

Following Eq. (9), the results for the Λ_b^0 cross-section measurements for $2.2 < y < 4.5$ and $p_T < 13.0$ GeV/c for the eight data samples considered are shown in Fig. 6.

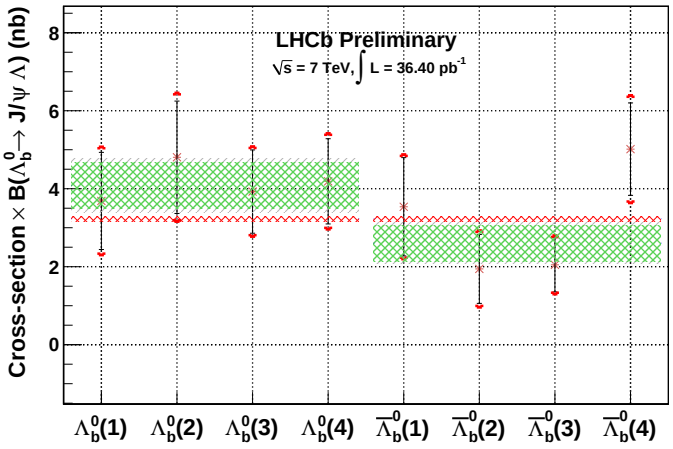

Figure 6: The measured $\sigma(pp \to \Lambda_b^0 X)\mathcal{B}(\Lambda_b^0 \to J/\psi\Lambda^0)$ in nb for the eight samples. The black vertical bars represent the statistical error, the red limits represent the systematic uncertainty. The green horizontal band represents the average for the two species Λ_b^0 and $\bar{\Lambda}_b^0$. The red horizontal line represents the predictions from the LHCb simulated sample. (1)&(2) stand for the measurement using Λ_b^0 reconstructed with Λ^0 daughters as long tracks using data recorded with different polarity of the magnetic field, while (3)&(4) stand for the case in which the Λ^0 daughters are reconstructed as downstream tracks.

The Λ_b^0 and $\bar{\Lambda}_b^0$ production cross-sections are obtained as the weighted average of the individual samples assuming full correlation of the systematic uncertainties:

$$\sigma(pp \to \Lambda_b^0 X)\mathcal{B}(\Lambda_b^0 \to J/\psi\Lambda^0) = 4.08 \pm 0.59(stat) \pm 0.36(syst)\,\text{nb},$$

$$\sigma(pp \to \bar{\Lambda}_b^0 X)\mathcal{B}(\bar{\Lambda}_b^0 \to J/\psi\bar{\Lambda}^0) = 2.60 \pm 0.46(stat) \pm 0.26(syst)\,\text{nb}.$$

The values are in reasonable agreement with the LHCb Monte Carlo predictions, also shown in Fig. 6. They also agree qualitatively with the CMS measurement [27], however a quantitative comparison is difficult, given the different y and p_T ranges covered by the two experiments. The results from this analysis have been presented in a public conference [6] and also an internal [7] and a public document [8] were written.

6 Conclusions and outlook

In the first part of this thesis we have looked on some of the aspects of SM, perturbative Quantum Chromodynamic and the current framework for making predictions on b quark production at LHCb. Also we made a short description of LHCb experiment. The second part of the thesis is dedicated to the original results. They consist of a method for obtaining calibration samples for the RICH detector, a complete data analysis of the measurement of Λ_b cross-section production, and a software package available for further use.

The results from this thesis improve the knowledge of heavy baryon systems, subject which was less accessible and studied in the past. Foreseeable extensions of the analysis notwithstanding the better investigation of the Λ_b spectra, are in the direction of studying the fragmentation fractions and their possible dependency of energy, in the investigation of heavier baryons or in the rare decays field. All the results from this thesis have been presented publicly in papers and conferences.

Acknowledgments

I would like to warmly thank to my supervisor dr. Sabin Stoica for his permanent guidance and for giving me the opportunity to work in such a large and "beautiful" collaboration as LHCb. I have met there many interesting and dedicated people which helped me shape my understanding on the current problems in particle physics. I mention here Olivier Schneider, Guy Wilkinson, Tatsuya Nakada who guided my participation in the CERN working groups. Special thanks are due to my collaborators Raluca Muresan and Marco Adinolfi who helped me with the intricacies of LHCb software and the studies from this thesis. Also, I would like to thank to all my colleagues from LHCb-Ro group for many interesting discussions about LHCb subjects and to my colleagues from DFT department for their support and understanding.

This thesis was financed by the Romanian National Authority for Scientific Research (ANCS), mainly through the "Capacitati" Program

which supports the Romanian participation at CERN.

Output publications from the thesis

[1] B. Popovici and S. Stoica, *Calibration of LHCb RICH detectors with $\Lambda \to p\pi$ decay using data*, (Physics at LHC 2008, Split), Split University, Sep, 2008. http://marjan.fesb.hr/physicslhc/.

[2] LHCb Collaboration, B. Popovici *et al.*, *Prompt K^0_s production in pp collisions at $\sqrt{s} = 0.9$ TeV*, Phys. Lett. **B693** (2010) 69, arXiv:1008.3105.

[3] LHCb Collaboration, B. Popovici *et al.*, *Measurement of V^0 production ratios in pp collisions at $\sqrt{s} = 0.9$ and 7 TeV*, JHEP **1108** (2011) 034, arXiv:1107.0882.

[4] LHCb Collaboration, B. Popovici *et al.*, *Measurement of prompt hadron production ratios in pp collisions at $\sqrt{s} = 0.9$ and 7 TeV*, Eur. Phys. J. **C72** (2012) 2168, arXiv:1206.5160.

[5] LHCb Collaboration, B. Popovici, *Particle production studies at LHCb*, Acta Phys. Polon. **B42** (2011) 1547, LHCb-PROC-2011-021, CERN-LHCb-PROC-2011-021.

[6] B. Popovici, *b hadron production at LHCb*, (2012 LHC days in Split), Split University, 01-06.10, 2012. LHCb-TALK-2012-282, http://lhc2012.fesb.hr/index.php.

[7] LHCb collaboration, B. Popovici, R. Mure'san, and M. Adinolfi, *Measurement of the $\Lambda_b \to J/\Psi\Lambda^0$ production cross-section in pp collisions at $\sqrt{s} = 7$ TeV*, , internal note, Linked to LHCb-CONF-2012-031.

[8] LHCb collaboration, B. Popovici, M. Adinolfi *et al.*, *Studies of $\Lambda^0_b \to J/\psi\Lambda$ production in pp collisions at $\sqrt{s} = 7$ TeV*, , public note, Linked to LHCb-ANA-2011-106.

References to scientific literature

[1] ATLAS Collaboration, G. Aad *et al.*, *Observation of a new particle in the search for the Standard Model Higgs boson with the ATLAS detector at the LHC*, Phys. Lett. **B716** (2012) 1, arXiv:1207.7214; CMS Collaboration, S. Chatrchyan *et al.*, *Observation of a new boson at a mass of 125 GeV with the CMS experiment at the LHC*, Phys. Lett. **B716** (2012) 30, arXiv:1207.7235.

[2] W. Hollik, *Quantum field theory and the Standard Model*, arXiv:1012.3883.

[3] P. Nason, S. Dawson, and R. K. Ellis, *The Total Cross-Section for the Production of Heavy Quarks in Hadronic Collisions*, Nucl. Phys. **B303** (1988) 607.

[4] P. Nason, S. Dawson, and R. K. Ellis, *The One Particle Inclusive Differential Cross-Section for Heavy Quark Production in Hadronic Collisions*, Nucl. Phys. **B327** (1989) 49.

[5] M. Cacciari and M. Greco, *Large p_T hadroproduction of heavy quarks*, Nucl. Phys. **B421** (1994) 530, arXiv:hep-ph/9311260.

[6] M. Cacciari, M. Greco, and P. Nason, *The P(T) spectrum in heavy flavor hadroproduction*, JHEP **9805** (1998) 007o, arXiv:hep-ph/9803400.

[7] T. Sjöstrand, S. Mrenna, and P. Skands, *PYTHIA 6.4 physics and manual*, JHEP **05** (2006) 026, arXiv:hep-ph/0603175; T. Sjostrand, S. Mrenna, and P. Z. Skands, *A Brief Introduction to PYTHIA 8.1*, Comput. Phys. Commun. **178** (2008) 852, arXiv:0710.3820.

[8] M. Bahr *et al.*, *Herwig++ Physics and Manual*, Eur. Phys. J. **C58** (2008) 639, arXiv:0803.0883.

[9] T. Gleisberg *et al.*, *Event generation with SHERPA 1.1*, JHEP **0902** (2009) 007, arXiv:0811.4622.

[10] P. Nason, *A New method for combining NLO QCD with shower Monte Carlo algorithms*, JHEP **0411** (2004) 040, arXiv:hep-ph/0409146; S. Frixione, P. Nason, and C. Oleari, *Matching NLO QCD computations with Parton Shower simulations: the POWHEG method*, JHEP **0711** (2007) 070, arXiv:0709.2092; S. Alioli, P. Nason, C. Oleari, and E. Re, *A general framework for implementing NLO calculations in shower Monte Carlo programs: the POWHEG BOX*, JHEP **1006** (2010) 043, arXiv:1002.2581.

[11] J. L. Rosner, *Non-factorizable effects in top quark production*, Phys. Rev. **D86** (2012) 014011, arXiv:1205.1529.

[12] V. Bednyakov, G. Lykasov, and V. Lyubushkin, *Forward production of beauty baryons in pp collisions at LHC*, Europhys. Lett. **92** (2010) 31001, arXiv:1005.0559.

[13] LHCb collaboration, A. A. Alves Jr. *et al.*, *The detector at the LHC*, JINST **3** (2008) S08005.

[14] V. Gligorov, C. Thomas, and M. Williams, *The HLT inclusive B triggers*, LHCb-PUB-2011-016.

[15] R. Brun and F. Rademakers, *ROOT: An object oriented data analysis framework*, Nucl. Instrum. Meth. **A389** (1997) 81.

[16] I. Belyaev *et al.*, *Handling of the generation of primary events in , the simulation framework*, Nuclear Science Symposium Conference Record (NSS/MIC) **IEEE** (2010) 1155.

[17] D. J. Lange, *The EvtGen particle decay simulation package*, Nucl. Instrum. Meth. **A462** (2001) 152.

[18] P. Golonka and Z. Was, *PHOTOS Monte Carlo: a precision tool for QED corrections in Z and W decays*, Eur. Phys. J. **C45** (2006) 97, arXiv:hep-ph/0506026.

[19] GEANT4 collaboration, J. Allison *et al.*, *Geant4 developments and applications*, IEEE Trans. Nucl. Sci. **53** (2006) 270; GEANT4 collaboration, S. Agostinelli *et al.*, *GEANT4: A simulation toolkit*, Nucl. Instrum. Meth. **A506** (2003) 250.

[20] M. Clemencic *et al.*, *The simulation application, : design, evolution and experience*, J. of Phys. : Conf. Ser. **331** (2011) 032023.

[21] J. Podolanski and R. Armenteros, *Iii. analysis of v-events*, Philosophical Magazine Series 7 **45** (1954), no. 360 13, arXiv:http://www.tandfonline.com/doi/pdf/10.1080/14786440108520416.

[22] LHCb collaboration, *b-hadron lifetime measurements with exclusive $b \to j/\psi x$ decays reconstructed in the 2010 data*, , LHCb-CONF-2011-001.

[23] M. Pivk and F. R. Le Diberder, *sPlot: A statistical tool to unfold data distributions*, Nucl. Instrum. Meth. **A555** (2005) 356, arXiv:physics/0402083.

[24] J. A. Hernando Morata *et al.*, *Measurement of trigger efficiencies and biases*, Tech. Rep. CERN-LHCb-2008-073, Mar, 2010.

[25] M. Ferro-Luzzi, *Proposal for an absolute luminosity determination in colliding beam experiments using vertex detection of beam-gas interactions*, Nucl. Instrum. Meth. **A553** (2005) 388; LHCb collaboration, R. Aaij *et al.*, *Absolute luminosity measurements with the LHCb detector at the LHC*, JINST **7** (2012) P01010, arXiv:1110.2866.

[26] Particle Data Group, J. Beringer *et al.*, *Review of particle physics*, Phys. Rev. **D86** (2012) 010001.

[27] CMS Collaboration, S. Chatrchyan *et al.*, *Measurement of the Lambda(b) cross section and the $\bar{\Lambda}_b$ to Λ_b ratio with $\Lambda_b \to J/\psi\Lambda$ decays in pp collisions at $\sqrt{s} = 7$ TeV*, Phys. Lett. **B714** (2012) 136, arXiv:1205.0594.